Solvent Exchange Method for Protein-Based Bioplastics

Bam Manitsirisuk

A thesis

submitted in partial fulfillment of the
requirements for the degree of

Master of Science in Applied Chemical Science and Technology

University of Washington

2025

Committee:

Alshakim Nelson

Matthew Golder

Program Authorized to Offer Degree:
Department of Chemistry

University of Washington

Abstract

Solvent Exchange Method for Protein-Based Bioplastics

Bam Manitsirisuk

Chair of the Supervisory Committee:

Alshakim Nelson

Department of Chemistry

Additive manufacturing (AM) has seen significant growth in tissue engineering and medical device applications, with bioplastics emerging as preferred materials due to their biocompatibility and environmental sustainability. However, these bioplastic systems typically contain high water content, presenting significant challenges during the drying process. The high water content leads to anisotropic shrinkage, resulting in undesirable bending and warping of

printed structures, which compromises their dimensional accuracy and functional properties. This study investigates the optimization of solvent exchange protocols using ethanol to produce dimensionally stable prints from bovine serum albumin (BSA) and poly(ethylene glycol) diacrylate (PEGDA) resin through vat photopolymerization. Our methodology focuses on establishing precise drying procedures that maintain the structural integrity of the printed components while preserving their mechanical properties. The results demonstrate that solvent-exchanged samples exhibited less than 30% volume reduction compared to control samples, indicating superior dimensional stability. Mechanical characterization revealed that the solvent exchange process did not significantly alter the material's mechanical properties, suggesting the preservation of its structural functionality. Thermal analysis was conducted to quantify the residual water content in solvent-exchanged samples, providing insights into the effectiveness of the dehydration process. Furthermore, complex printed structures subjected to the optimized solvent exchange protocol showed significantly reduced shrinkage, bending, and warping compared to untreated samples. This work establishes a robust methodology for producing high-resolution, dimensionally stable BSA-PEGDA prints suitable for consistent mechanical testing and complex structure fabrication, potentially advancing the field of biofabrication for tissue engineering and medical device applications.

ACKNOWLEDGEMENTS

I would like to express my deepest gratitude to the Department of Chemistry at the University of Washington, and to the many individuals who have shaped and supported my journey toward a Master's degree.

Above all, I am profoundly thankful to my advisor, Professor Alshakim Nelson. His guidance, patience, and encouragement were foundational—not only to my development as a researcher but also to my ability to navigate the challenges of graduate school. I am truly fortunate to have had his mentorship. The Nelson Lab became a second home during these years, and the people within it defined my experience. I thank every member of the group for the camaraderie, shared effort, and lasting memories. I am especially grateful to Dr. Naroa Sadaba and Siwei Yu for their mentorship. Entering the lab with limited experience, I relied deeply on their clarity, patience, and generosity as I found my footing.

To Meijing Zhang—thank you for being my closest friend and constant companion throughout this journey. From our first days in orientation to shared coursework, joining the same lab, and working side by side in the same subgroup, you were there through every stage. We learned, grew, and endured together. Your presence made all the difference, and it was an honor to work with you. To Jimin, Jennifer, and Sahana—thank you for your friendship, encouragement, and presence. You brought perspective and laughter when it was most needed, and helped make this experience far more meaningful. I wish each of you the very best in your own journeys ahead.

Finally, to my dearest parents and family—thank you for your unwavering love, belief, and support. Through every difficulty and moment of doubt, your presence sustained me. I owe this accomplishment to you.

Table of Contents

Chapter 1 Introduction..... 1

1.1 Additive Manufacturing 1

Classification of AM technologies: 3

1.2 Vat Photopolymerization..... 4

1.3 Protein-based Biomaterials 6

Bovine Serum Albumin (BSA)..... 7

Protein-based Biomaterial for 3d-printing..... 8

1.4 BSA-PEGDA 10

Chapter 2: Solvent Exchange..... 12

Section 1: Background 12

2.1 Additive manufacturing for Biomaterials..... 12

2.2 Solvent Exchange 12

2.2 Solvent Effects on Polymer-Protein Systems..... 14

2.3 Post processing methods..... 17

2.4 Research objective..... 19

Section 2: Materials & Experimental Procedures 20

2.5 List of Chemicals..... 20

2.6 Experimental procedures 20

Section 3: Results and Discussion..... 22

2.7 Processing and Fabrication..... 22

2.8 Mechanical Analysis (Tensile) 29

2.9 FTIR Characterization 31

2.10 Thermal Characterization 33

Conclusion: 36

Future Work:..... 37

List of Figures

Chapter 1

Figure 1.1 Classification of AM techniques[6] 4

Figure 1.2 Schematic illustrating material composition for vat polymerization process, which can be either a pure resin or advanced material, such as ceramic or metal suspensions, which can be added and mixed with the resin before printing[10] 5

Figure 1.3 Schematic representation of BSA-PEGDA resin preparation.[19] 10

Chapter 2

Figure 2.1 Schematic representation of protein-based biomaterials air drying vs. solvent exchange 19

Figure 2.2 Drying Procedure for (A) Control sample (B) Solvent exchanged sample (C) Control HT sample (D) Solvent exchanged HT Sample 21

Figure 2.3 Visual comparison of BSA-PEGDA flat sheets processed by solvent exchange (left) and bench drying (right) over two days. Each row shows samples imaged on Day 1 (first column) and Day 2 (second column) to assess changes in shrinkage and warping over time 24

Figure 2.4 Qualitative comparison between bending angle of solvent exchange vs. bench drying sample 25

Figure 2.5 Comparison of interlocking ring structures demonstrating shape retention. (A) Original CAD models used for 3D printing. (B) Air-dried control samples after 2 days. (C) Ethanol-treated samples (90% EtOH, 2-day drying). Top and side views are shown for each condition. 26

Figure 2.6 Comparison between the 9x9x9 mm lattice original CAD model (A) printed BSA-PEGDA lattice structures after bench drying (B) and solvent exchange in 90% ethanol (C). Solvent exchange better preserves the intended geometry compared to bench drying. 27

Figure 2.7 Volume and mass change for printed bars 29

Figure 2.8 Tensile result of BSA/PEGDA 3:1, BSA/PEGDA 3:1 HT, BSA/PEGDA 3:1EtOH90%, BSA/PEGDA 3:1 EtOH90% HT..... 31

Figure 2.9 FTIR Spectra of BSA/PEGDA 3:1, BSA/PEGDA 3:1 HT, BSA/PEGDA 3:1EtOH90%, BSA/PEGDA 3:1 EtOH90% HT..... 33

List of Tables

Table 1. Printing parameters of BSA/PEGDA 3:1 22

List of Equations

1. Volume Change 27

2. Mass Change 28

List of Abbreviations

Abbreviation	Definition
AM	Additive Manufacturing
BSA	Bovine Serum Albumin
PEGDA	Poly(ethylene glycol) diacrylate
DLP	Digital Light Processing
EtOH	Ethanol
HT	Heat Treatment

Chapter 1 Introduction

1.1 Additive Manufacturing

Additive Manufacturing (AM), commonly known as 3D printing, represents a transformative approach to fabrication where physical objects are created directly from digital designs. This revolutionary process offers significant advantages over conventional manufacturing methods, particularly in terms of production efficiency and flexibility[1]. AM has experienced substantial development since its introduction in the 1980s. Originally intended for rapid prototyping, it has evolved into a reliable and versatile manufacturing approach used across various industries. Advances in material science, processing technologies, and digital design tools have played a key role in expanding its applications to sectors such as aerospace, automotive, healthcare, and fashion[2]. AM is now recognized for its ability to produce highly customized components, minimize material waste, and fabricate complex geometries that are often impractical with conventional manufacturing methods[3]. This progress has established AM as a diverse set of processes capable of working with polymers, metals, ceramics, and composite materials, which contributes significantly to innovation across multiple fields. AM has gained significant interest in both industry and academia, with its market projected to reach $96.7 billion by 2030, growing at a compound annual growth rate (CAGR) of 21% between 2024 and 2030[4]. Particularly, the polymer segment of additive manufacturing is projected to grow to USD 23.15 billion by 2033, with an expected compound annual growth rate (CAGR) of 8.25% over the forecast period from 2025 to 2033[5].

The AM workflow consists of three primary stages: digital design, model preparation, and physical fabrication. Initially, a three-dimensional digital model is created using Computer-

Aided Design (CAD) software and saved in a stereolithography (STL) format. This digital blueprint is then processed through specialized software that segments the model into precise, printable layers. During this "slicing" phase, the complex geometries of the CAD model are approximated using triangular meshes, generating detailed instructions for each printed layer. Finally, these instructions guide the 3D printer in depositing material layer by layer to construct the physical object[6].

The technology's advantages are multifaceted. AM enables unprecedented design customization, allowing objects to be tailored to specific requirements without additional tooling costs. It significantly reduces material waste compared to subtractive manufacturing methods, as material is added only where needed. Furthermore, AM opens new possibilities in design complexity and functionality, enabling the creation of intricate structures that would be impossible or impractical to produce through traditional methods.

As an emerging technology, AM shows promise in high-value applications across various sectors. It has gained significant traction in aerospace engineering, medical device manufacturing, and scientific research, where its ability to produce complex, customized components with high precision offers compelling advantages. As technology continues to mature, it may increasingly supplement or replace traditional manufacturing processes, especially for applications requiring intricate geometries, customization, or small production runs.

Classification of AM technologies:

The ISO/ASTM 52900 standard classifies additive manufacturing in seven process categories: binder jetting, directed energy deposition, material extrusion, material jetting, powder bed fusion, sheet lamination and vat polymerization (Figure 1.1). As AM is used in wide industries with different purposes, each different kind of printer is used for different kinds of material. In additive manufacturing, the choice of material is closely tied to the printing process, as each technology supports specific classes of materials with unique processing requirements[7]. For instance, material extrusion techniques such as Fused Deposition Modeling (FDM) commonly use thermoplastics like PLA and ABS due to their ease of melting and solidification. Powder bed fusion methods work predominantly with metals (e.g., titanium, stainless steel) or polymers (e.g., nylon), while binder jetting can be applied to sand, ceramics, or metal powders. Vat photopolymerization (VP), which includes processes like SLA and DLP, primarily utilizes liquid photopolymer resins that solidify under light exposure[1]. This category has garnered growing interest, particularly in the development of bio-based and biodegradable resins, due to its compatibility with high-resolution applications and expanding use in biomedical and sustainable materials research.

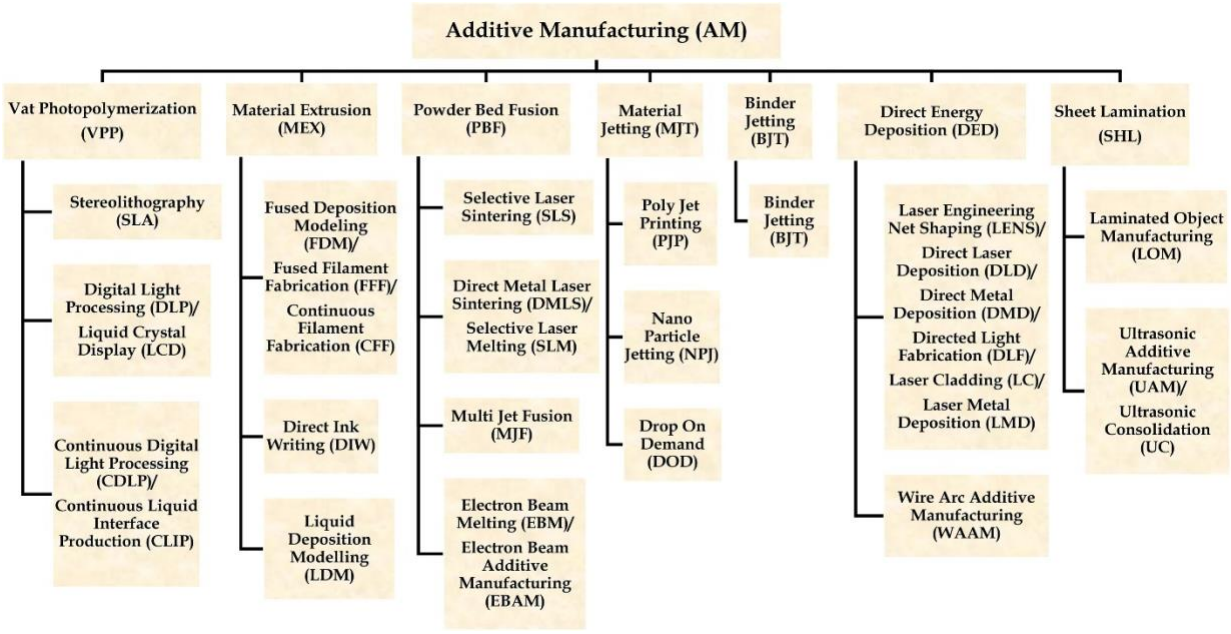

Figure 1.1 Classification of AM techniques[6]

1.2 Vat Photopolymerization

Vat photopolymerization (VP) is one of the popular techniques in AM where it uses a light source to cure photocurable resin. This technology has many variants, such as digital light printing (DLP), stereolithographic apparatus (SLA), mask projection SL (MPSL), microstereolithography (μSL), and two-photon polymerization (TPP)[8]. However, the most commonly used techniques are DLP, SLA and TPP as it allows for an easy set up and fast production[9]. The advantage of VP is that it is very fast and could cure resin with high precision and results with good resolution. This characteristic is important for applications that require precise geometries and shapes such as tissue engineering, blood vessels, or even artistic designs.

Among the various vat photopolymerization (VP) techniques, Digital Light Processing (DLP) offers a compelling combination of high resolution, rapid fabrication speed, and cost-efficiency, making it particularly attractive for biofabrication and microstructure printing. Unlike

point-by-point methods such as stereolithography (SLA), DLP utilizes a Digital Micromirror Device (DMD) to project a sequence of two-dimensional light patterns onto a photosensitive resin, thereby polymerizing entire layers in parallel. This parallel processing significantly reduces printing time while preserving fine structural detail and surface quality. Each projected image is composed of pixels defined by an array of individually tilting micromirrors within the DMD. The size and arrangement of these mirrors directly influence the resolution in the XY plane, as they determine the pixel density of each exposed layer[10].

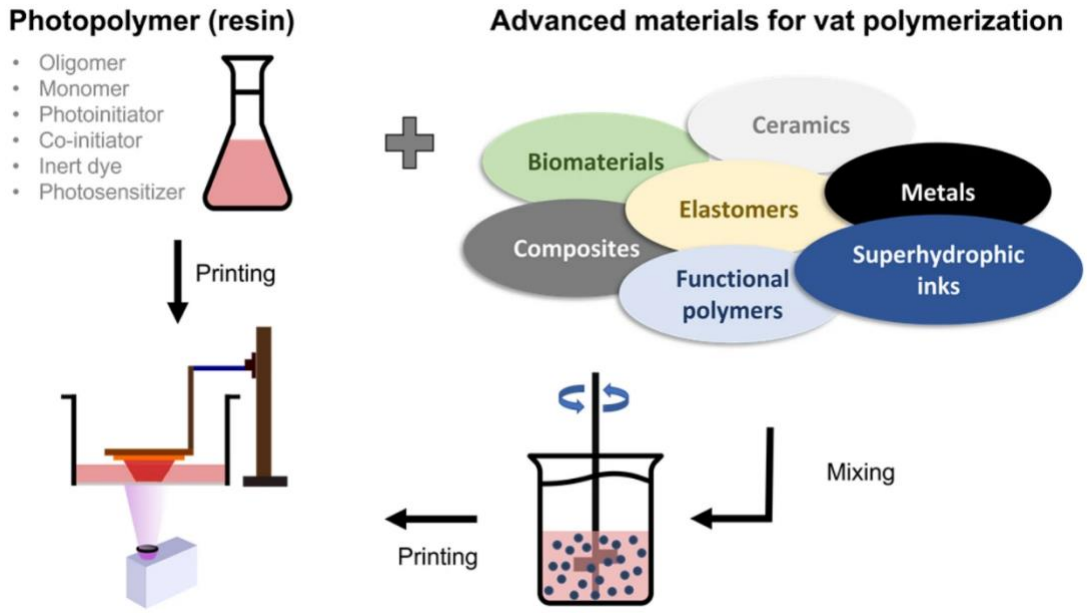

Figure 1.2 Schematic illustrating material composition for vat polymerization process, which can be either a pure resin or advanced material, such as ceramic or metal suspensions, which can be added and mixed with the resin before printing[10]

As for all the VP types of printers, all of them have almost the same set up, which includes a light source, a resin tray, and a printer head. The light source is typically a UV laser light source, which shines the light through to the resin tray. Then there is a build head that

moves up and down in a Z-direction, trapping a layer of liquid resin into each layer depending on the thickness parameter[10]. Figure 1.2 shows a schematic flow diagram of how the DLP printing process works.

1.3 Protein-based Biomaterials

Protein-based biomaterials have emerged as promising alternatives to conventional petroleum-based materials. These environmentally friendly, versatile, and biodegradable materials consist of high protein content and minimal polymer additives, making them increasingly attractive for sustainable applications. What makes protein-based biomaterials distinct from conventional polymeric materials is that they are sourced from sustainably grown renewable resources. Some criteria for these types of materials are that they are produced using environmentally friendly manufacturing processes, safe and non-hazardous for the environment, reused and recycled at the end of their intended use, such as feedstock for another process or via recycling or composting[11].

In the past years, studies have been using different kinds of protein such as casein, whey, gelatin, and soy for cooperation with polymers to create a distinct protein material for desired applications[8]. However, there are still drawbacks from these kinds of protein since some of them possess fast degradation, batch-to-batch variations, or big quantity availability[12,13].

Proteins are complex macromolecules composed of linear chains of amino acids linked by peptide bonds. Each amino acid contributes its unique structure to the protein backbone, resulting in a wide range of sizes, shapes, and chemical properties. Based on their morphology, proteins are commonly classified as either fibrous or globular. Fibrous proteins, such as collagen, keratin, and elastin, have elongated, thread-like structures that primarily serve structural or

mechanical roles and are typically water-insoluble due to their repetitive sequences and extended conformations. In contrast, globular proteins, including enzymes, antibodies, and serum albumin, adopt compact, spheroid configurations with hydrophobic interiors and hydrophilic exteriors, making them soluble in aqueous environments.[14]

The choice to use globular proteins for biomaterial development is motivated by their favorable solubility, chemical versatility, and structural complexity, all of which are critical for applications such as hydrogels, drug delivery systems, and bioplastics. Their solubility allows for easy processing in aqueous media, while their diverse amino acid compositions and folded structures, rich in α-helices and β-sheets, provide tunable interactions and mechanical properties.[15] These features enable globular proteins to form functional biomaterials that can retain water, interact with other biomolecules, and be readily crosslinked or modified.[16] By leveraging these properties, globular proteins offer a robust platform for designing responsive and adaptable biopolymeric systems.

Bovine Serum Albumin (BSA)

BSA is a globular protein extracted from cows, with a structure resembling the heart-like shape of human serum albumin (HSA). Composed of 583 amino acid residues, BSA has a molecular weight of approximately 66.5 kDa and contains 67% alpha helix with no beta sheets[16]. At 25 °C in water, BSA has an isoelectric point of 4.7, contributing to its high water solubility[7]. The protein features lysine residues positioned on its surface, making these charged amino acids accessible to external molecules and facilitating molecular interactions.

BSA has been used in various types of applications ranging from drug delivery systems to material chemistry. A work by Wang and Zhang showed the use of BSA as drug carrier, surface

engineering and biomimetic synthesis for cancer imaging and therapy[17]. Holt et al. used BSA as a biocompatible dispersant for single-wall carbon nanotubes (SWCNTs), enabling their individual dispersion in water while preserving their optical properties and facilitating cellular uptake without toxicity[18]. Also, in the field of material science, Sanchez et al. uses Polyethylene glycol diacrylate (PEGDA) to functionalize with BSA through aza-michael addition to create a shape memory protein-based biomaterial[19].

Protein-based Biomaterial for 3D-printing

The field of additive manufacturing has been using conventional polymer materials such as PLA, PET, or PVC for filaments or resin. However, these materials have a relatively slow degradation lifespan. Therefore, protein/protein-based material has been an alternative constituent for additives in polymeric materials.

There are some criteria for choosing a protein of choice in these materials. They must be sourced from renewable resources, stable from batch-to-batch, and cost effective in order to be used in real-world applications. Some common proteins that have been used previously in the field of 3d-printing are collagen, gelatin, keratin, fibrin, and BSA[20].

Various proteins serve as building blocks for biomaterial applications, each with distinct characteristics that determine their suitability for specific biomedical applications[16]. Collagen, the most abundant extracellular matrix protein in mammals, constitutes approximately 35% of total protein content and features a primary sequence of repeating peptide units (Gly-X-Y), where X and Y are often proline or hydroxyproline. While its structural organization provides excellent mechanical properties, the telopeptide domains represent the most immunogenic regions of collagen[12,21,22]. Although enzymatic removal of these domains can reduce

immunogenicity in purified preparations, this approach is not feasible for tissue-based biomaterials since these regions serve as critical crosslinking sites. Alternative immunogenicity reduction methods include glutaraldehyde crosslinking, though this introduces additional considerations regarding cytotoxicity.

Gelatin, a denatured form of collagen not found in nature but obtained through hydrolytic processing, offers improved processability despite reduced mechanical strength. This characteristic makes gelatin particularly valuable for 3D printing applications, where its thermal responsiveness enables structural stability after printing. Keratin, abundant in feathers, wool, and hair, exists in two structural categories: alpha-types exhibiting helical structures with 7 nm diameter and beta-types forming beta-sheet structures with 3 nm diameter. The high cysteine content in keratin facilitates extensive disulfide bond formation, providing exceptional stability but simultaneously contributing to poor aqueous solubility, which limits its processability for certain biomaterial application[13].

Fibrin, a nanofibrous protein involved in blood clotting and wound healing, provides a natural scaffold that supports cellular activities during tissue regeneration. However, its crosslinked form presents technical challenges for extrusion-based fabrication methods, particularly in 3D printing applications[23,24]. In contrast, BSA offers distinctive advantages that address many limitations encountered with other protein-based materials. Derived from cows, BSA features an almost complete absence of heterologous groups on its surface, which is predominantly composed of lysine residues. This composition creates a generally hydrophilic surface chemistry that promotes excellent solubility and processability without requiring extensive modifications. Additionally, the abundance of lysine residues provides numerous sites for controlled chemical modification and crosslinking, allowing precise tuning of material

properties for specific applications. These combined characteristics make BSA an optimal choice for developing biomaterial systems that require precise control over physical, chemical, and biological properties, positioning it as the protein of choice for our research focus.

1.4 BSA-PEGDA

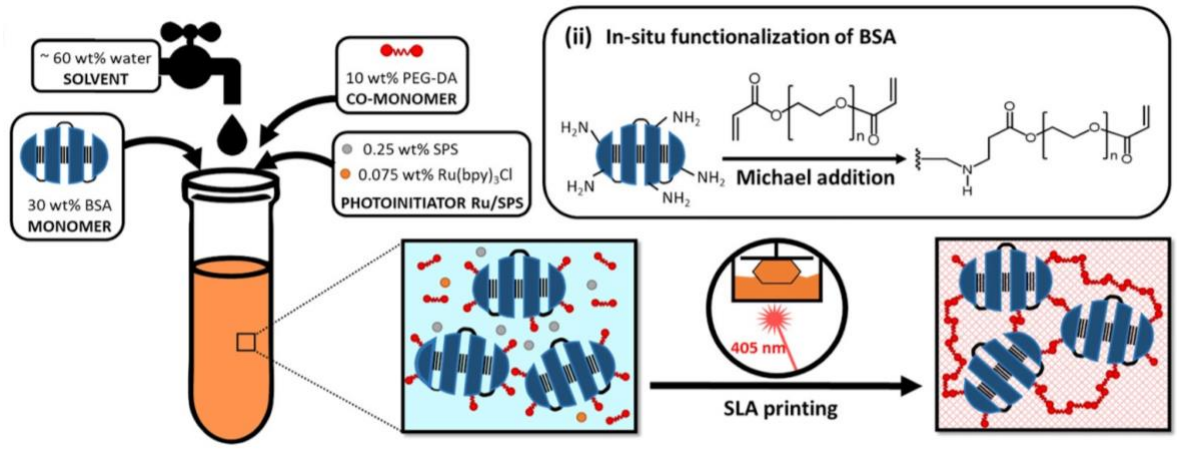

Figure 1.3 Schematic representation of BSA-PEGDA resin preparation.[19]

Poly(ethylene glycol) diacrylate or PEGDA is a derivative from polyethylene glycol (PEG) that is widely used in the field of creating hydrogels. It consists of diacrylate groups at the chain end which could gel rapidly at room temperature with the presence of photo initiator and light. Nowadays, it is a good candidate to make bioplastic or hydrogel in the field of AM.

As mentioned previously, Sanchez et.al. has created a shape memory protein-based biomaterial. This particular material is made up of BSA as a protein and PEGDA as the polymer. In this work, PEGDA was functionalized in-situ with BSA through aza-Michael addition where the acrylate chain ends reacted with the lysine surface of BSA (Figure 1.3). This generates a BSA-functionalized PEGDA solution. Upon adding photo initiator, whether it's

tris(bipyridine)ruthenium(II) chloride with sodium persulfate (Ru/SPS) or lithium phenyl-2,4,6-trimethylbenzoylphosphinate (LAP), and UV curing, the free acrylate groups will crosslink with each other to form a hydrogel network. And therefore, we get a BSA-PEGDA network in a hydrogel state. Since the BSA-PEGDA network is made up of a high amount of water after UV-curing and it is in its hydrogel state, there are high chances that water could leave the system during drying into a bioplastic state[25]. This consequently could affect the mechanical properties internally and externally and causes the desired structure to bend/warp and shrink from the original structure[11].

Chapter 2: Solvent Exchange

Section 1: Background

2.1 Additive manufacturing for Biomaterials

Additive Manufacturing (AM) is a fabrication technique that creates objects by depositing material layer by layer. Nowadays bio-based resins have gained attention in this field due to their potential for biomedical applications. Among the various 3D printing methods, vat photopolymerization is often preferred for protein-based bioplastics. This technique involves the use of a liquid resin that is cured layer by layer through light exposure.

Protein-based resins typically incorporate a photoinitiator, making them suitable for digital light processing (DLP) or stereolithography (SLA) printing. In this work, a BSA-PEGDA resin is prepared by adding a photoinitiator and then printed using a DLP printer. During the printing process, the projected light selectively cures the resin, building the structure layer by layer according to the digital design.

2.2 Solvent Exchange

Solvent exchange has emerged as a powerful technique in biomaterial fabrication, where it offers precise control over microstructures and material properties beyond conventional manufacturing methods. This process involves the rapid solidification of polymer structures through controlled solvent-non-solvent interactions, enabling the creation of precisely engineered materials with unique structural and functional characteristics. In industrial applications, solvent exchange techniques such as Solvent Exchange Deposition Modeling (SEDM) have been utilized to fabricate micro-sized, flexible PLGA scaffolds for skin substitutes by directly printing PLGA dissolved in N-methyl pyrrolidone into ethanol at room temperature[26]. Similarly, solvent-

exchange-assisted direct ink writing has overcome limitations of traditional solvent-evaporation techniques in creating accurate and stable 3D polyvinylidene fluoride piezoelectric energy harvesters, enabling complete retention of filament measurements while generating beneficial micropores and promoting specific phase crystallization[27,28]. However, despite these advances, solvent exchange has been predominantly explored in the context of hydrogels, often employing critical drying techniques to freeze structures and create micropores. The application of solvent exchange methodologies to bioplastics remains comparatively underexplored, representing a significant gap in current research. This limited exploration of solvent exchange in bioplastic systems presents valuable opportunities for extending these techniques beyond conventional hydrogel applications, potentially enabling novel microstructural control and functional properties in sustainable bioplastic materials that could address pressing challenges in fields ranging from medical devices to environmental remediation.

2.2 Solvent Effects on Polymer-Protein Systems

Polymer–Solvent Interactions

Hydrogels contain a high percentage of water, which can cause network collapse or anisotropic shrinkage when dried conventionally into bioplastics. Solvent exchange offers an alternative drying method that helps preserve structural integrity. This technique is commonly employed to introduce porous structures into hydrogel networks, enhancing mechanical properties and facilitating the preparation of aerogels and xerogels. One such method is critical point drying, where the hydrogel is frozen to extremely low temperatures under CO_2 conditions. This process removes solvents while maintaining a uniform porous network structure, preventing collapse during conventional drying methods[29].

A variety of solvents can be used in the solvent exchange process of hydrogels. However, amphiphilic solvents are often favored due to their ability to penetrate both hydrophilic and hydrophobic regions of the polymer network. Ethanol (EtOH) is commonly preferred among these solvents due to its small molecular size, amphiphilic nature, and relatively low boiling point[30]. These properties make ethanol highly effective at diffusing into PEGDA hydrogels, facilitating the replacement of water and other solvents without compromising the polymer network structure.

When ethanol interacts with PEGDA hydrogels, it can promote temporary disruption of the water-bound network, leading to physical changes such as swelling or partial collapse depending on concentration and exposure time[31–33]. Ethanol's rapid evaporation rate further supports efficient drying, preserving porosity and microstructural integrity[34]. Additionally, ethanol is often used in solvent-induced phase separation (SIPS) to create macroporous structures that enhance the mechanical properties and swelling behavior of PEGDA hydrogels. Hydrogels

fabricated via SIPS with ethanol demonstrate increased storage modulus (G′), indicating enhanced stiffness compared to those prepared with aqueous precursors [35,36].

Furthermore, ethanol's amphiphilic nature supports uniform solvent exchange throughout both hydrophilic and hydrophobic domains of the PEGDA matrix, helping retain structural integrity during dehydration and promoting mechanical performance tailored to specific applications[37].

Protein–Solvent Interactions: Ethanol and BSA

In protein-based systems such as BSA–PEGDA hydrogels, ethanol presents a dual role. While it facilitates drying and structural stabilization, ethanol can also disrupt protein structure due to its chaotropic nature. Ethanol exposure has been shown to induce conformational changes in BSA, leading to partial or full denaturation in a concentration-dependent manner. These structural alterations are supported by changes in spectroscopic properties[38].

Moreover, ethanol affects BSA's binding characteristics, particularly its interaction with fatty acids. It has been observed to reduce the fraction of strongly bound fatty acids in BSA hydrogels by up to 52%, potentially altering the protein's role in the matrix and affecting its stability [37]. Ethanol-induced denaturation can also lead to aggregation or loss of solubility, thereby impacting the functional and mechanical properties of the hydrogel.

Therefore, careful optimization of ethanol concentration during solvent exchange is essential. While too much ethanol may lead to protein denaturation and material deformation, controlled use allows for efficient water removal, porosity preservation, and partial retention of BSA bioactivity[37].

Role of water in material properties

Protein-based bioplastics incorporate substantial quantities of water that functions as an essential binding medium for the polymer-protein network architecture. The progressive dehydration of these materials inevitably leads to dimensional instability as water molecules gradually evacuate the system through evaporation. This water loss disrupts the internal network configuration through anisotropic shrinkage, whereby the material contracts non-uniformly across different axes. These heterogeneous contractions manifest as visible distortions in both the surface topography and macroscopic morphology of the bioplastic construct, where it compromises the structural fidelity and its functional performance.

Water significantly influences the mechanical properties of polymeric materials. Higher water content increases chain mobility within the polymer network by reducing intermolecular forces, resulting in enhanced flexibility. Water acts as an effective plasticizer by forming hydrogen bonds with both the polymer chains and protein components, further facilitating molecular movement. However, this increased elasticity comes with a trade-off, while the material becomes more flexible, its overall strength may decrease. Materials with high water content typically exhibit lower young's modulus due to the loosened network structure, though they demonstrate superior elongation capabilities before failure[39].

Purpose of Solvent Exchange in hydrogels/biomaterial

In recent days, many studies have been using solvent exchange methods to create macroporous materials within a hydrogel to achieve higher mechanical properties for many applications such as thermal super insulators to scaffold for regenerative medicine[26]. Many hydrogels are known for high water uptake, which is known as a medium to create a loose network. However, upon drying the hydrogel turned into a bioplastic, these materials tend to

have a collapse network, which could potentially affect the mechanical properties. Therefore, solvent exchange method is an alternative way that is used to preserve the internal structure of the hydrogel to create a macroporous structure to keep its functionality while in dehydration state. The most common method that was used is supercritical drying, where hydrogels are prepared first prior to solvent exchange and then sent to freeze dry under CO_2.

2.3 Post processing methods

Post-processing refers to the set of techniques applied to improve the surface finish and overall quality of printed objects after fabrication. The specific methods used vary depending on the printing technology and material involved. For example, fused deposition modeling (FDM) often utilizes paper sanding to achieve a smoother surface. Among the different additive manufacturing methods, vat photopolymerization (VP) typically requires the most extensive post-processing due to the nature of the resin-based printing process.

After objects are printed using VP techniques, residual uncured resin invariably remains on the surface, which requires dedicated post-processing steps to achieve optimal finish quality. In contemporary additive manufacturing, industry leaders such as Formlabs, Anycubic, and Prusa have developed sophisticated post-processing protocols that typically involve UV curing, treatment with anhydrous industrial alcohols, and mechanical refinement through paper sanding to produce defect-free printed objects with superior surface characteristics[40].

Among the solvents commonly employed in the post-processing workflow, anhydrous alcohol such as Isopropyl alcohol (IPA) and ethanol (EtOH) have gained widespread usage due to their commercial availability and economic feasibility[41]. IPA has emerged as the industry-

preferred option owing to its cost-effectiveness and ubiquitous availability in the markets. Additionally, specialized solvents like Tripropylene glycol monomethyl ether (TPM) have been commercialized by numerous companies as alternative cleaning agents[42]. These solvents demonstrate excellent capability in dissolving commercial photopolymer resins without initiating undesirable chemical interactions that might compromise the integrity of the resin's internal or external polymeric network structure[43].

In stark contrast to the well-established post-processing protocols for conventional photopolymer resins, the post-processing method for protein-based resins remains largely unexplored in the field of biofabrication. Most research studies employing protein-based resins have predominantly relied on simple finishing techniques such as air-drying or direct UV curing to solidify and stabilize the printed structures. However, this approach presents significant challenges when applied to protein-based formulations, particularly those based on BSA-PEGDA systems, which inherently contain substantial quantities of water in their composition.

The high water content in protein-based resins introduces complex drying dynamics that can significantly impact on the structural integrity of printed objects. During conventional air-drying processes, water evaporation occurs unevenly throughout the printed structure, inducing anisotropic shrinkage of the polymeric network (Figure 2.1). This differential contraction generates internal stresses that manifest as macroscopic warping or bending of the printed object. This dimensional distortion represents a critical challenge in the field, as the functional utility of 3D printed objects across various applications fundamentally depends on their ability to replicate the dimensional specifications and geometric features of the original digital design.

The development of specialized post-processing methodologies tailored specifically for protein-based resins therefore represents a crucial research frontier that must be addressed to

unlock the full potential of these biomaterials in advanced manufacturing applications where dimensional accuracy and structural fidelity are the key requirements.

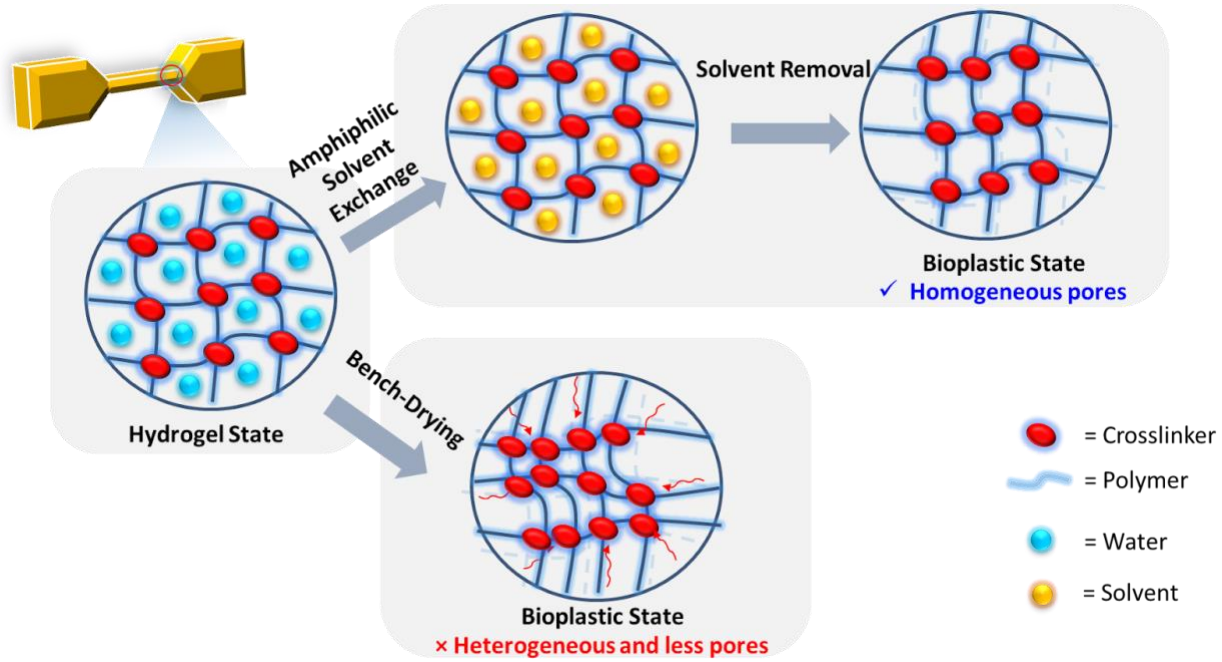

Figure 2.1 Schematic representation of protein-based biomaterials air drying vs. solvent exchange

2.4 Research objective

The objective of this research is to develop solvent exchange methods/drying procedures to produce warp-free BSA-PEGDA resin prints for reliable mechanical testing. Where the approach is to replace water with solvent, explore the effect of solvent exchange on the material's mechanical property, and to prevent the printed structure from bending/warping.

Section 2: Materials & Experimental Procedures

2.5 List of Chemicals

Bovine serum albumin was purchased from Proliant. Poly(ethylene glycol diacrylate) 575, Lithium Bromide, and ethyl acetate was purchased from Sigma-Aldrich. Dimethyl phenylphosphonite, 2,4,6-Trimethylbenzoyl Chloride was purchased from TCI America. Ethanol was obtained from Fischer Scientific.

2.6 Experimental procedures

2.6.1 Preparation of LAP

Lithium Phenyl (2,4,6-Trimethylbenzoyl) Phosphinate (LAP) is prepared by mixing (0.018 mol) of dimethyl phenylphosphonite and (0.018 mol) 2,4,6-trimethylbenzoyl chloride (under Nitrogen). The reaction was left stirred for 18 hours. Then, Lithium Bromide and Ethyl acetate (excess) was added and heated up to 50°C for 10 minutes to precipitate the reaction. The precipitated product was filtered, crude, and checked with NMR before usage.

2.6.2 Preparation of BSA/PEGDA Resin

The resin formulation used is 40% solid content is used and 60% of water. The ratio between protein and polymer used in this experiment was a 3:1 ratio of BSA/PEGDA. For each batch of samples, 20 grams of resin were made. BSA was added with water first, vortex until BSA is fully dissolved, then PEGDA is added after. The reaction mixture is left on the bench for 24 hours to let the BSA and PEGDA react, then LAP is added before 3D printing.

2.6.3 Drying Procedure

The drying procedure is a procedure of preparing samples after printing. For our control samples (BSA/PEGDA 3:1), the printed structure is bench dried on a drying rack for 2 days prior to doing any mechanical test. In our solvent exchanged samples (BSA/PEGDA-Ethanol) The printed structure is directly swelled in ethanol for 1 day, followed by bench drying 1 day before testing (Figure 2.2).

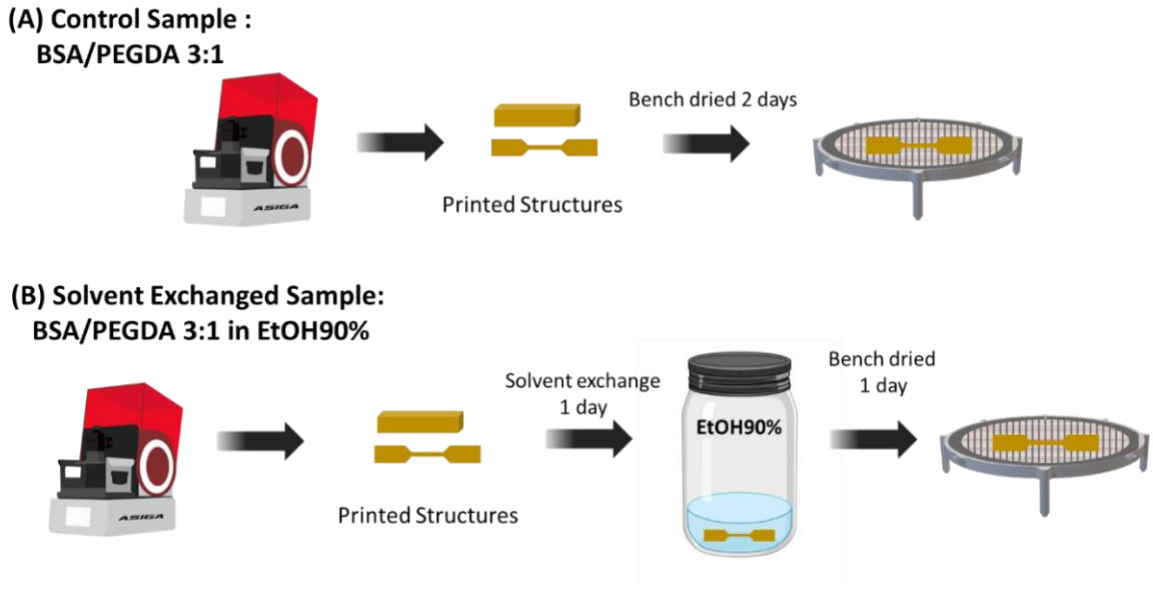

Figure 2.2 Drying Procedure for (A) Control sample (B) Solvent exchanged sample

2.6.4 Preparation of Tensile Test Specimens

Tensile tests were performed with a TestResources 100 Series Universal uniaxial tension with 1 kN load cells at a speed of 1 mm/min until mechanical failure. Preparing for tensile test specimens, the resin prints are printed from Asiga max mini (DLP printer) in dogbone shapes following an ISO 527-2 (ISO 527-2/5B/6) standard.

Section 3: Results and Discussion

2.7 Processing and Fabrication

2.7.1 Optimization of DLP Printing Parameters for BSA/PEGDA

Optimizing the printing parameter is very crucial since it's the first step that is used to prepare samples. A slight change of exposure time, layer height, and print orientation can greatly impact the final print quality. These factors influence surface finish, accuracy, mechanical strength, and overall part functionality, making it crucial to fine-tune them for each specific print job and material to achieve the desired results.

The printer that was used in this work is the Asiga max mini (Din). Where the light intensity used is 20.00 cm/s. Burn-in-layer and exposure is 1.00 second per scan and built plate separation distance is 1.00 mm/s (Table 1).

Table 1. Printing parameters of BSA/PEGDA 3:1

Settings	**Adjusted Parameters**
Light intensity	20.0 cm/second
Burn-in-layer	1.00 second/scan
Built plate separation distance	1.00 mm/second

Visual Comparison of Bench-dried vs Solvent Exchanged Samples

2.7.2 Surface Quality and Dimensional Accuracy

We printed flat sheets with a thickness of 1.00 mm, matching our dogbone specimens, to evaluate dimensional stability during drying. This thickness was chosen deliberately as it allows

air to penetrate the samples more easily than thicker structures, making any warping tendencies readily apparent.

After the initial drying process (Figure 2.3) we observed striking differences between the two preparation methods. The solvent-exchanged samples remained flat with no visible distortion along the edges. In contrast, bench-dried samples showed obvious bending, particularly along the lower left corner. This warping indicates that water evaporated unevenly from the bench-dried samples, causing anisotropic shrinkage of the polymer network. The solvent-exchanged samples appeared to maintain a more uniform network alignment throughout.

To assess stability over time, we continued observations for two days after initial drying. The solvent-exchanged samples preserved their original flat geometry with no evidence of warping. Meanwhile, bench-dried samples showed progressive deterioration in shape fidelity, with increased bending extending to the top right corner. These results strongly suggest that solvent exchange effectively prevents the uneven internal stresses that typically develop during conventional air drying of hydrogel structures, resulting in superior dimensional accuracy of the final parts.

Figure 2.4 compares the deformation of BSA-PEGDA printed bar samples between untreated controls and samples subjected to solvent exchange in 90% ethanol. In the control samples (top row), noticeable bending was observed, with recorded angles of 3.51° and 2.85°, indicating a slight but consistent warping behavior. In contrast, the solvent-exchanged samples (bottom row) exhibited much lower bending angles of 0.19° and 0.27°, suggesting that solvent exchange treatment reduced the extent of deformation. Although this example demonstrates a clear reduction in bending after solvent exchange, it should be noted that direct comparison across different batches is challenging because warping does not consistently occur at the same

location on the samples. Therefore, while solvent exchange appears to mitigate bending in this instance, more controlled and positionally consistent studies would be necessary to fully quantify this effect.

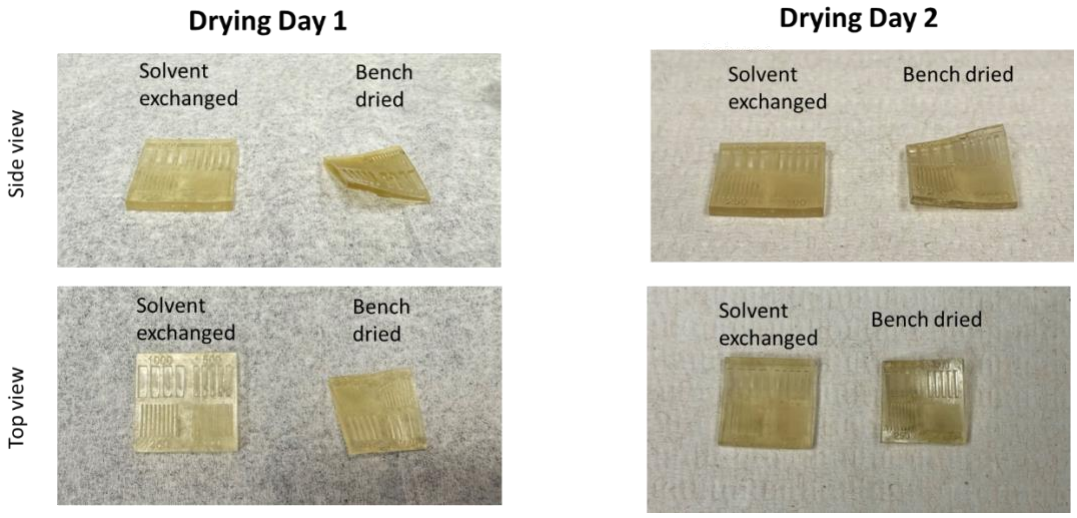

Figure 2.3 Visual comparison of BSA-PEGDA flat sheets processed by solvent exchange (left) and bench drying (right) over two days. Each row shows samples imaged on Day 1 (first column) and Day 2 (second column) to assess changes in shrinkage and warping over time

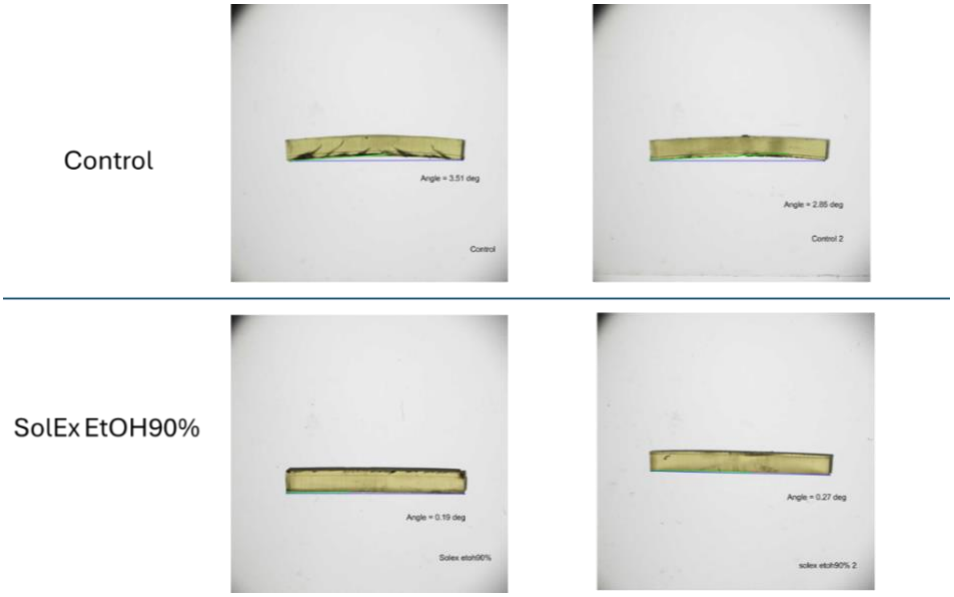

Figure 2.4 Qualitative comparison between bending angle of solvent exchange vs. bench drying sample

To further validate our findings, we fabricated a more intricate structure with interlocking rings designed to test shape retention properties under different drying conditions (Figure 2.5). This complex geometry represents structures commonly encountered in practical applications that require difficult prints. The results clearly demonstrate that the ethanol-treated sample (EtOH 90% dried for 2 days) maintained remarkable fidelity to the original design, preserving both the circular profile and spatial relationships between the interlocking components. In contrast, the control sample (air-dried for 2 days without solvent exchange) exhibited significant deformation and structural collapse, this demonstrates that it is unsuitable for precise applications

Another example (Figure 2.6) shows the original CAD model (left) alongside BSA-PEGDA printed lattice structures that were either bench-dried (middle) or solvent-exchange in 90% ethanol (right). Because of the thin line thickness in the lattice design, maintaining the

printed structure's shape was challenging. The bench-dried sample shows significant bending and distortion, with visible collapse of the lattice compared to the original model. In contrast, the solvent-exchanged sample more closely preserves the intended geometry, with strut alignment and overall form better matching the CAD design. These results suggest that solvent exchange helps stabilize thin-walled structures, reducing deformation that would otherwise occur during drying. This comparison provides compelling evidence that our solvent exchange protocol is essential for maintaining geometric accuracy in complex 3D-printed structures with accurate features.

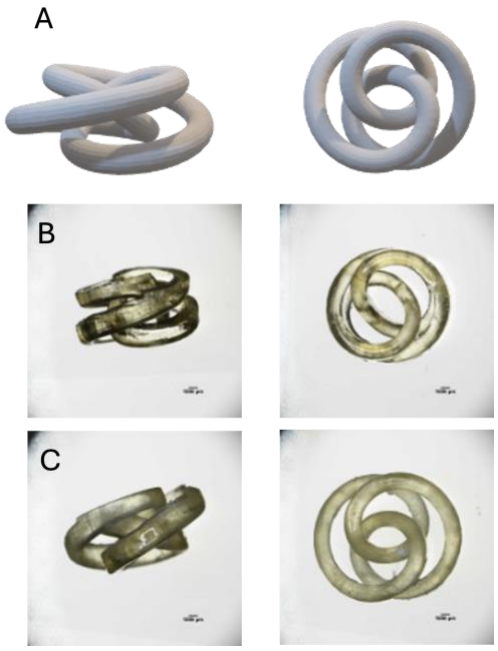

Figure 2.5 Comparison of interlocking ring structures demonstrating shape retention. (A) Original CAD models used for 3D printing. (B) Air-dried control samples after 2 days. (C) Ethanol-treated samples (90% EtOH, 2-day drying). Top and side views are shown for each condition.

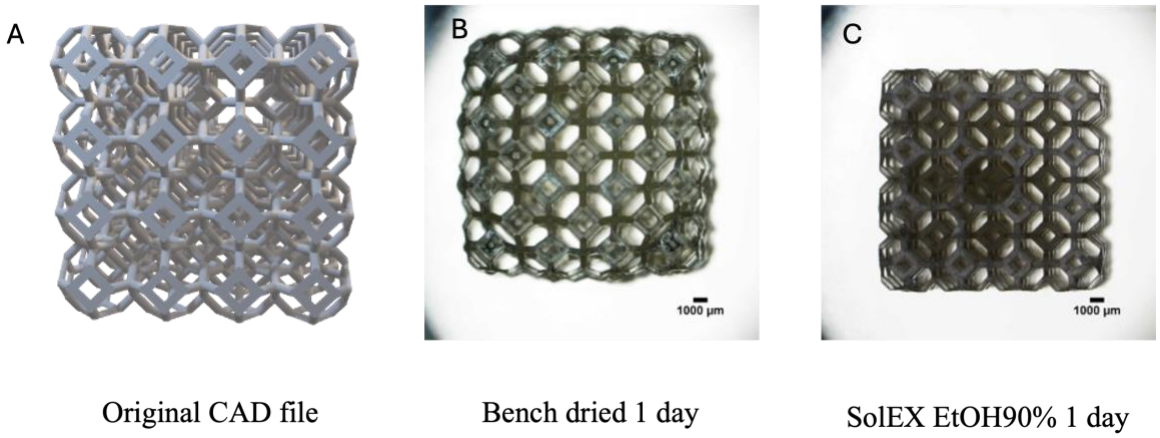

Figure 2.6 Comparison between the 9x9x9 mm lattice original CAD model (A) printed BSA-PEGDA lattice structures after bench drying (B) and solvent exchange in 90% ethanol (C). Solvent exchange better preserves the intended geometry compared to bench drying.

2.7.3 Solvent Exchange Process

During solvent exchanging, the original concentration used is EtOH100%. However, after the exchange process, the dogbones still bent to a high degree. This suggests that the exchange rate of EtOH100% is too rapid, causing the network to shrink anisotropically and that leads to bending/warping. By this, we decrease the concentration of the solvent to EtOH90% with 10% water %v/v to slow the exchange rate of the solvent and water in the network. Prior to changing the solvent concentration, surface observation based, the dogbones do not bend or warp and result with an accurate structure as printed.

1. Volume Change

$$\textbf{Volume change} = \frac{\mathbf{V_{final}} - \mathbf{V_{initial}}}{\mathbf{V_{final}}} \times \mathbf{100} \quad (1)$$

To see the surface level of how solvent exchanging could preserve the structure of the printed sample, we observe the dimensional changes in volume of the printed sample based on (Equation 1). The samples were printed in bars with dimensions of 20x5x2 mm. The bars were measured in its initial dimension right after printing. Consequently, the final volume was measured after solvent exchange for 1 day. As a result, Control samples have lost 60% volume change while for EtOH90% samples have lost 22% samples. This could show that control samples have lost all the water content after drying, which corresponds to the amount of water used in the resin formulation. While for EtOH90% samples, the volume change shows a small difference, showing that it could preserve the dimensions to an extent and the shrinkage is much lesser compared to our control sample. However, for heat treated samples, both of the control heated and EtOH90% heat shows the same volume decrease around 60% meaning that most of the contents left in the sample are the solid content and that water and solvent has been removed from the samples (Figure 2.7).

2. Mass Change

$$\textbf{Mass change} = \frac{\mathbf{W_{final} - W_{initial}}}{\mathbf{W_{final}}} \times \mathbf{100} \quad (2)$$

Prior to volume change, we also conducted mass change to observe the trend to see if the mass of the object corresponds to the shrinkage in dimension of the sample (Equation 2). As a result, the mass change correlates with the volume change. EtOH90% sample has 28% changes in the final volume from the initial volume, while all the other samples have almost 60% changes

(Figure 2.7). This could confirm that the trend of shrinkage is reliable since the mass trend also aligns with it.

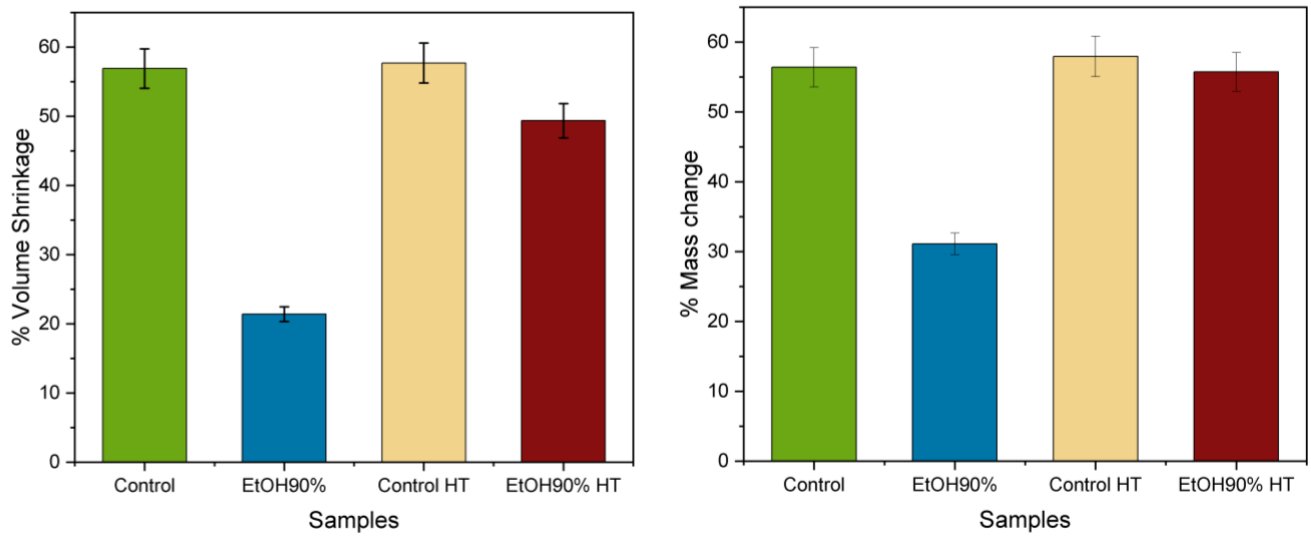

Figure 2.7 Volume and mass change for printed bars

To better understand how solvent exchange affects mechanical properties, we conducted uniaxial tensile testing on our samples. The control samples had a Young's modulus of about 617.8 ± 12.70 MPa, while the samples treated with 90% ethanol (EtOH90%) showed a modulus of 367.8 ± 9.80 MPa—about 30% lower than the control. This suggests that while solvent exchange does weaken the material, the effect is not drastic. The reduction in stiffness could be due to ethanol acting as a plasticizer, making the material more flexible but slightly less tough.

Interestingly, the elongation at break, or how much the material stretches before breaking, was significantly higher in the EtOH90% samples. They stretched on average 148.74 ± 10.9%, which is about 40% more than the control samples (89.7 ± 8.4%). This increased stretchability could be due to two factors. First, some residual ethanol and water likely remained in the

network, softening the material and increasing mobility. Second, the solvent exchange may have introduced larger pores into the structure. In contrast, the control samples, which were dried on a bench, became denser and more compact, reducing their ability to stretch.

After heat treatment (HT), we saw a major increase in stiffness for both the control and ethanol-treated samples. Their Young's modulus doubled, likely due to changes in the protein's structure. In BSA-based materials, heat treatment tends to unfold α-helices into β-sheets, which act like reinforcing structures. This makes the material significantly tougher but also less elastic. The HT control samples had a modulus of 1045 ± 46.4 MPa, while HT EtOH90% samples reached 810.9 ± 56.2 MPa. The difference between them was only about 20%, suggesting that ethanol treatment didn't significantly alter the mechanical properties after heat exposure.

However, once heat-treated, nearly all residual solvent and water were removed, making the material much more brittle. As a result, the elongation at break dropped drastically. HT control samples only stretched 7.9%, and HT EtOH90% samples stretched 15.5% before breaking.

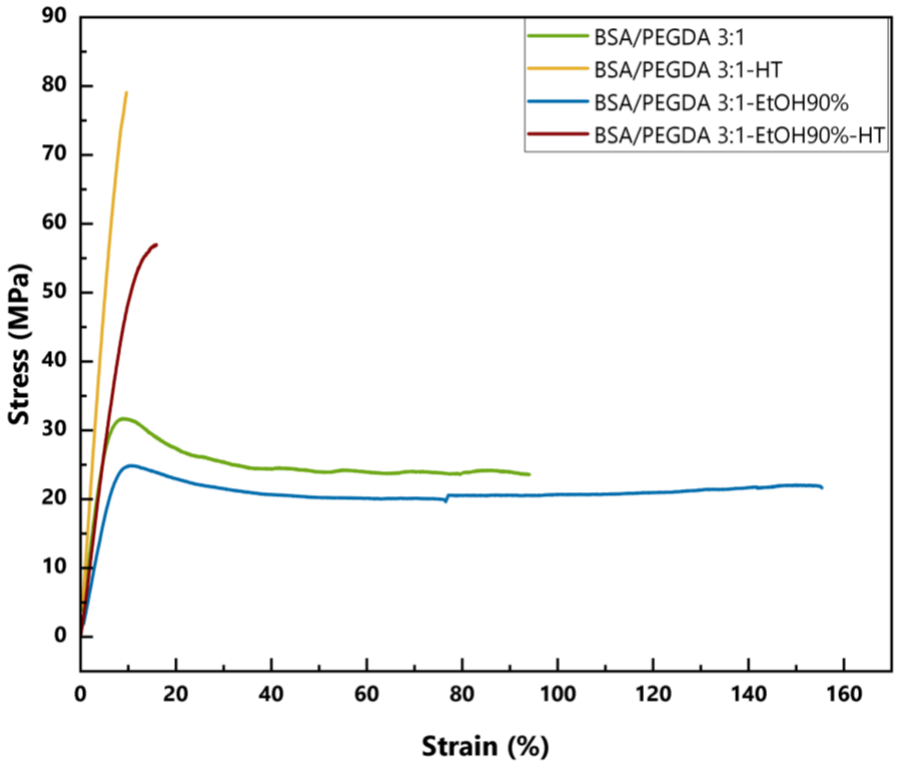

Figure 2.8 Tensile result of BSA/PEGDA 3:1, BSA/PEGDA 3:1 HT, BSA/PEGDA 3:1EtOH90%, BSA/PEGDA 3:1 EtOH90% HT

2.9 FTIR Characterization

To explain the results obtained from tensile analysis, we use FTIR (Fourier transform infrared spectroscopy) to see the relationship between the control samples, solvent exchanged samples and control heated, solvent exchanged heated samples. Based on our tensile results, the heat-treated samples showed 3-fold higher in young's modulus compared to our control samples. We believe that it is due to the changes of secondary structure in the protein upon heat treatment. 1640 cm^{-1} represents alpha helical segments of the BSA while 1622 cm^{-1} corresponds to the aggregated intermolecular beta-sheets[44]. Literature suggests that upon heating BSA at 74 °C will reveal the formation of significant irreversible beta aggregation of the protein[15].Therefore in this study, we wanted to use ftir to confirm the changes in secondary structure where alpha-helix has

been converted into beta sheets upon heat treatment. Based on the result (Figure 2.9), both heat-treated samples (BSA/PEGDA 3:1 HT and BSA/PEGDA-EtOH 90 % HT) showed a peak at 1622 cm^{-1}, which corresponds to β-sheet peaks that arose from unfolding of the protein. This finding dovetails with our mechanical data, where Young's modulus increases drastically owing to protein denaturation and the formation of β-sheet that physically reinforce the hydrogel network. Also, as mentioned previously, ethanol tends to favor partial unfolding of BSA under mild conditions. Recent ATR-IR and rheology work on ethanol-induced BSA gels showed that a shoulder at 1620 cm^{-1} grows gradually but remains smaller than in thermally denatured samples, and the resulting gels display only modest gains in storage modulus[45]. Our spectra manifests a slight peak at 1635 cm^{-1} feature in the solvent-exchanged (non-heated) sample, indicating that some α-helices have converted to β-sheets; however, the extent of conversion is limited, which corresponds to the tensile data where the modulus is not significantly increased compared to the fully heat-treated samples. Ultimately, FTIR confirms that the dramatic stiffening after thermal annealing is driven by a substantial increase in β-sheet content, whereas ethanol alone induces only partial unfolding and, by acting as a plasticizer, does not translate into a comparable mechanical reinforcement.

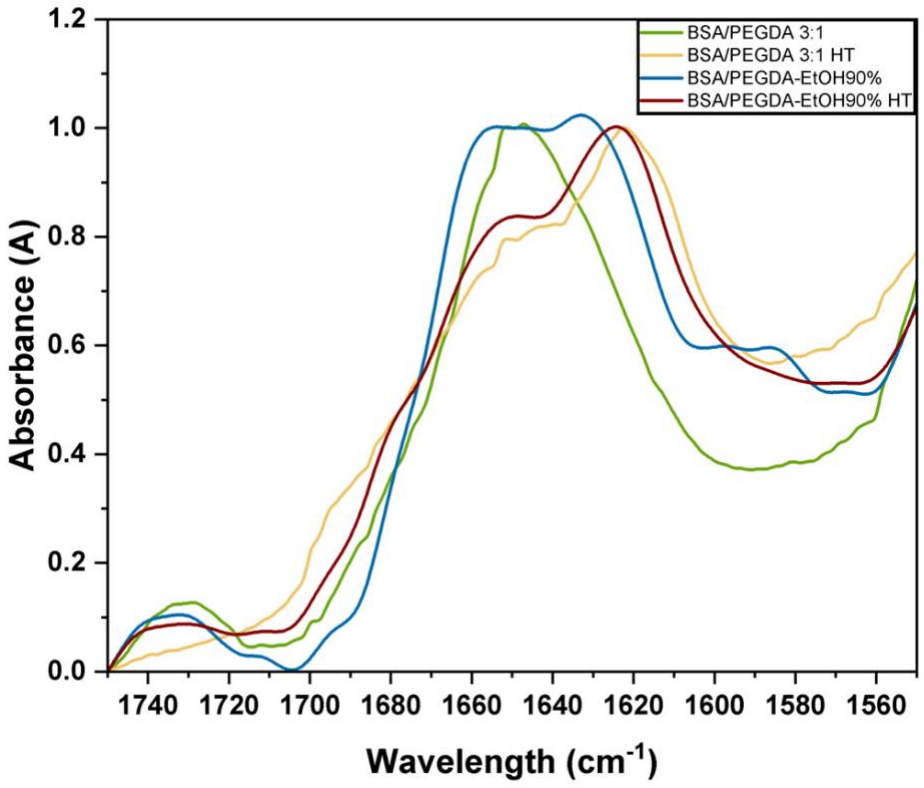

Figure 2.9 FTIR Spectra of BSA/PEGDA 3:1, BSA/PEGDA 3:1 HT, BSA/PEGDA 3:1EtOH90%, BSA/PEGDA 3:1 EtOH90% HT

2.10 Thermal Characterization

2.10.1 Residual Solvent/Water Content

To observe the composition of our sample, TGA (Thermogravimetric Analysis) was used to determine the amount of residual solvents and water. The test was ramped 10 °C/min isothermally at 100 °C since water's boiling point is 100 °C and ethanol is 78 °C. All the samples show different amounts of water content. Starting from control samples, there's only 3.09% of residual solvents in the sample, while EtOH90% sample shows 7.36%. This corresponds to our tensile data of the higher elasticity of the material. While for thermal treated samples, both

control and EtOH90% shows only 2.33% and 1.09% of residual solvent respectively, indicating that most of the solvent contents has been removed or evaporated prior to thermal treatment (Figure 2.10).

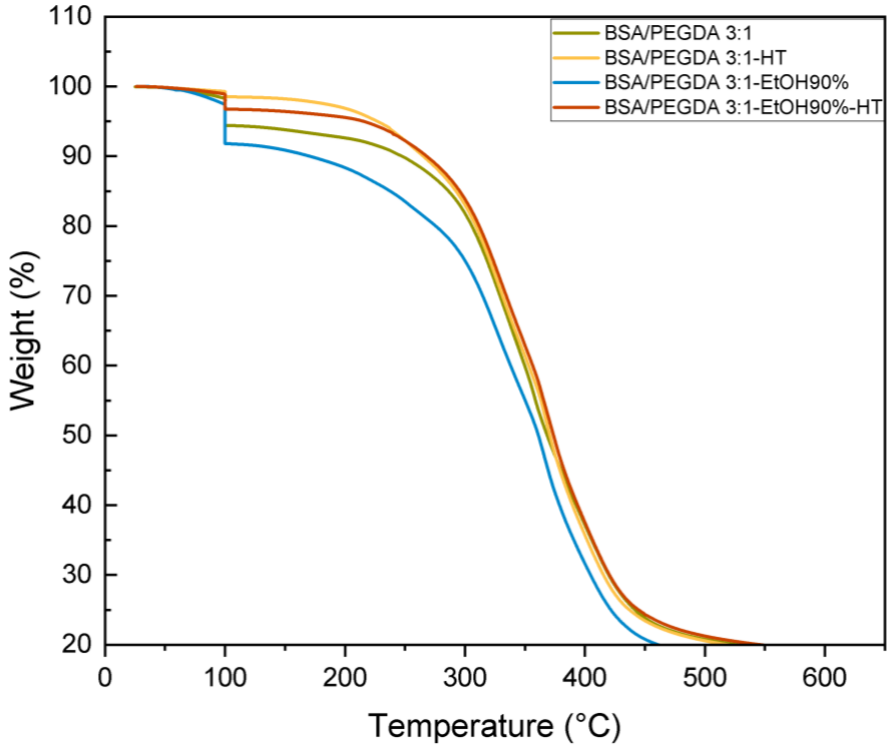

Figure 2.10 TGA Result of of BSA/PEGDA 3:1, BSA/PEGDA 3:1 HT, BSA/PEGDA 3:1EtOH90%, BSA/PEGDA 3:1 EtOH90% HT

2.10.2 Protein Denaturation

Furthermore, we used differential scanning calorimetry (DSC) to investigate how BSA responds to various treatments. Our DSC measurements compared untreated BSA with samples that underwent ethanol treatment (90%), heat treatment, or a combination of both (Figure 2.11).

The control BSA exhibited its typical endothermic peak around 100-120°C, which represents the protein unfolding from its native state. When treated with ethanol alone, BSA

showed a stronger denaturation peak at approximately 90°C. This shift suggests ethanol interacts with the protein structure, though not enough to cause complete denaturation on its own.

Most importantly, our heat-treated samples (both with and without ethanol) showed virtually no denaturation peaks at 90°C. This absence clearly indicates that the BSA had already denatured during our heat treatment protocol, before the DSC analysis was performed. The flat profile in this temperature range provides strong evidence of prior denaturation.

We observed that the combination of ethanol treatment followed by heat exposure produced the flattest thermogram, suggesting the most thorough denaturation. This points to ethanol making the protein more susceptible to heat-induced structural changes, likely by weakening the stabilizing forces within BSA's structure.

These findings confirm our hypothesis that our heat treatment successfully causes irreversible denaturation of BSA, and that ethanol pre-treatment enhances this effect.

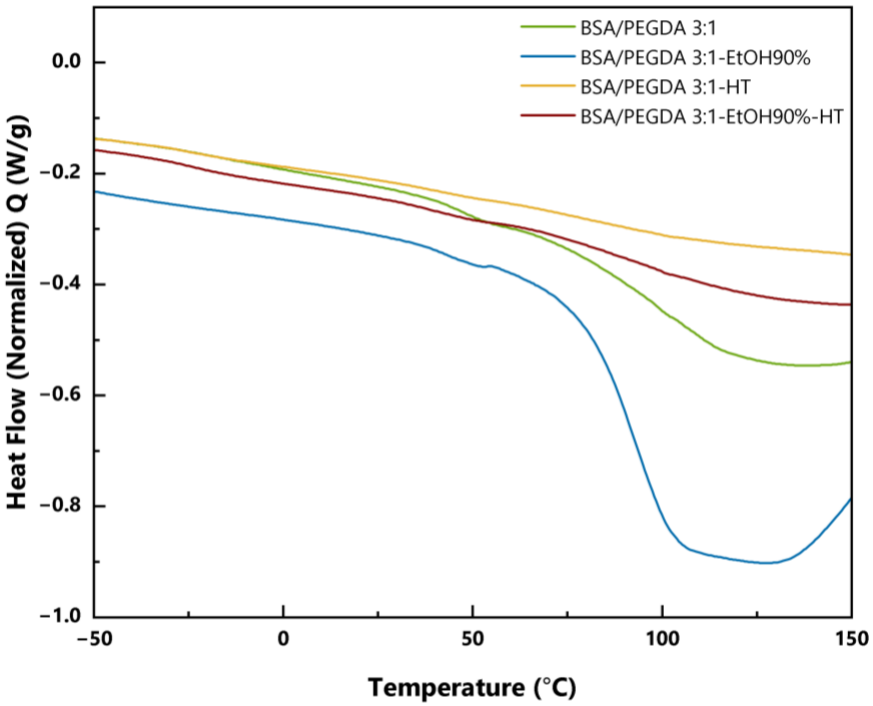

Figure 2.11 DSC result of BSA/PEGDA 3:1, BSA/PEGDA 3:1 HT, BSA/PEGDA 3:1EtOH90%, BSA/PEGDA 3:1 EtOH90% HT

Conclusion:

This study demonstrates the effectiveness of solvent exchange as a post-processing strategy to improve the dimensional stability and mechanical reliability of 3D-printed BSA-PEGDA bioplastics. By replacing water with 90% ethanol prior to drying, we successfully reduced warping and preserved the original printed geometry, even in complex structures. Solvent-exchanged samples showed significantly lower volume and mass shrinkage compared to control samples, indicating more uniform drying and network retention. Mechanical testing revealed that while ethanol treatment slightly reduced stiffness, it significantly increased elongation at break, suggesting enhanced flexibility due to residual solvent and a potentially more open microstructure. Heat treatment further reinforced the material, doubling the Young's modulus for both control and solvent-treated samples through protein structural transitions from α-helix to β-sheet formations. Complementary thermal and spectroscopic analyses confirmed

these structural changes and the role of ethanol in facilitating protein denaturation. Overall, this work presents solvent exchange as a simple yet promise method to improve print quality and consistency in protein-based resins.

Future Work:

While this study successfully demonstrated the effects of solvent exchange on dimensional stability and mechanical properties of BSA-PEGDA prints, further analysis is necessary to understand the underlying microstructural changes responsible for these improvements. This analysis will help clarify how the solvent exchange process alters the material's network structure compared to the control. By examining cross-sectional SEM images, we can visualize and compare pore size, distribution, and density between solvent-exchanged and bench-dried samples. This could provide direct evidence supporting the observed differences in mechanical flexibility and dimensional stability. It is hypothesized that solvent-exchanged samples retain more uniform and open porous networks, while control samples may exhibit denser, collapsed structures due to uneven water loss during drying. Understanding these microstructural differences will offer deeper insight into how solvent exchange contributes to warping prevention and mechanical performance.

Bibliography

1. Alexander, A. E.; Wake, N.; Chepelev, L.; Brantner, P.; Ryan, J.; Wang, K. C. A Guideline for 3D Printing Terminology in Biomedical Research Utilizing ISO/ASTM Standards. *3D Print. Med.* **2021**, *7* (1). https://doi.org/10.1186/s41205-021-00098-5.

2. Egon, A.; Bell, C.; Shad, R. Additive Manufacturing for Complex Geometries. *Preprints* **2024**, 2024072602. https://doi.org/10.20944/preprints202407.2602.v1

3. Dubey, D.; Singh, S. P.; Behera, B. K. A Review on Recent Advancements in Additive Manufacturing Techniques. *Proc. Inst. Mech. Eng., Part E: J. Process Mech. Eng.* **2024**, *0* (0). https://doi.org/10.1177/09544089241275860.

4. Everett, H. *AMPower Predicts 3D Printing Market to Be Worth €20bn by 2026 with PBF Leading the Way.* 3D Printing Industry. https://3dprintingindustry.com/news/ampower-predicts-3d-printing-market-to-be-worth-e20bn-by-2026-with-pbf-leading-the-way-206281/ (accessed May 1, 2025).

5. Polymer Additive Manufacturing Market Size, Share, Growth, Trends and Industry Analysis, By Type (Polymer Powder Bed Fusion, Vat Photopolymerization, Material Extrusion, Material Jetting, Binder Jetting), By Application (Transportation, Industrial, Life Sciences, Military and Aerospace, Consumer), Regional Insights and Forecast From 2025 to 2033. *Business Research Insights*, **2024**. https://www.businessresearchinsights.com/market-reports/polymer-additive-manufacturing-market-108180. (accessed April 26, 2025)

6. Wong, K. V.; Hernandez, A. A Review of Additive Manufacturing. *ISRN Mech. Eng.* **2012**, *2012* (1), 1–10. https://doi.org/10.5402/2012/208760.

7. Pérez, M.; Carou, D.; Rubio, E. M.; Teti, R. Current Advances in Additive Manufacturing. *Procedia CIRP* **2020**, *88*, 439–444. https://doi.org/10.1016/j.procir.2020.05.076.

8. Zhang, F.; Zhu, L.; Li, Z.; Wang, S.; Shi, J.; Tang, W.; Li, N.; Yang, J. The Recent Development of Vat Photopolymerization: A Review. *Addit. Manuf.* **2021**, *48* (102423), 102423. https://doi.org/10.1016/j.addma.2021.102423.

9. Lu, Z.; Gao, W.; Liu, F.; Cui, J.; Feng, S.; Liang, C.; Guo, Y.; Wang, Z.; Mao, Z.; Zhang, B. Vat Photopolymerization Based Digital Light Processing 3D Printing Hydrogels in Biomedical Fields: Key Parameters and Perspective. *Addit. Manuf.* **2024**, *94* (104443), 104443. https://doi.org/10.1016/j.addma.2024.104443.

10. Chaudhary, R.; Fabbri, P.; Leoni, E.; Mazzanti, F.; Akbari, R.; Antonini, C. Additive Manufacturing by Digital Light Processing: A Review. *Prog. Addit. Manuf.* **2023**, *8*, 331–351. https://doi.org/10.1007/s40964-022-00336-0.

11. Agnieray, H.; Glasson, J. L.; Chen, Q.; Kaur, M.; Domigan, L. J. Recent Developments in Sustainably Sourced Protein-Based Biomaterials. *Biochem. Soc. Trans.* **2021**, *49* (2), 953–964. https://doi.org/10.1042/bst20200896.

12. Veiga, A.; Silva, I. V.; Duarte, M. M.; Oliveira, A. L. Current Trends on Protein Driven Bioinks for 3D Printing. *Pharmaceutics* **2021**, *13* (9), 1444. https://doi.org/10.3390/pharmaceutics13091444.

13. Feroz, S.; Muhammad, N.; Ranayake, J.; Dias, G. Keratin-Based Materials for Biomedical Applications. *Bioact. Mater.* **2020**, *5* (3), 496–509. https://doi.org/10.1016/j.bioactmat.2020.04.007.

14. Widłak, W. Protein Structure and Function. *Mol. Biol.* **2013**, *8248*, 15–29. https://doi.org/10.1007/978-3-642-45361-8_2.

15. Vetri, V.; Librizzi, F.; Leone, M.; Militello, V. Thermal Aggregation of Bovine Serum Albumin at Different pH: Comparison with Human Serum Albumin. *Eur. Biophys. J.* **2007**, *36* (7), 717–725. https://doi.org/10.1007/s00249-007-0196-5.

16. Ge, S.; Kojio, K.; Takahara, A.; Kajiyama, T. Bovine Serum Albumin Adsorption onto Immobilized Organotrichlorosilane Surface: Influence of the Phase Separation on Protein Adsorption Patterns. *J. Biomater. Sci., Polym. Ed.* **1998**, *9* (2), 131–150. https://doi.org/10.1163/156856298x00479.

17. Wang, J.; Zhang, B. Bovine Serum Albumin as a Versatile Platform for Cancer Imaging and Therapy. *Curr. Med. Chem.* **2018**, *25* (25), 2938–2953. https://doi.org/10.2174/0929867324666170314143335.

18. Holt, B. D.; Dahl, K. N.; Islam, M. F. Quantification of Uptake and Localization of Bovine Serum Albumin-Stabilized Single-Wall Carbon Nanotubes in Different Human Cell Types. *Small* **2011**, *7* (16), 2348–2355. https://doi.org/10.1002/smll.201100437.

19. Sanchez-Rexach, E.; Smith, P. T.; Gomez-Lopez, A.; Fernandez, M.; Cortajarena, A. L.; Sardon, H.; Nelson, A. 3D-Printed Bioplastics with Shape-Memory Behavior Based on Native Bovine Serum Albumin. *ACS Appl. Mater. Interfaces* **2021**, *13* (16), 19193–19199. https://doi.org/10.1021/acsami.0c22377.

20. Mirzaei, M.; Okoro, O. V.; Nie, L.; Freitas, D.; Shavandi, A. Protein-Based 3D Biofabrication of Biomaterials. *Bioengineering* **2021**, *8* (4), 48. https://doi.org/10.3390/bioengineering8040048.

21. Włodarczyk-Biegun, M. K.; Del Campo, A. 3D Bioprinting of Structural Proteins. *Biomaterials* **2017**, *134*, 180–201. https://doi.org/10.1016/j.biomaterials.2017.04.019.

22. Lynn, A. K.; Yannas, I. V.; Bonfield, W. Antigenicity and Immunogenicity of Collagen. *J. Biomed. Mater. Res. B Appl. Biomater.* **2004**, *71* (2), 343–354. https://doi.org/10.1002/jbm.b.30096.

23. De Melo, B. A. G.; Jodat, Y. A.; Cruz, E. M.; Benincasa, J. C.; Shin, S. R.; Porcionatto, M. A. Strategies to Use Fibrinogen as Bioink for 3D Bioprinting Fibrin-Based Soft and Hard Tissues. *Acta Biomater.* **2020**, *117*, 60–76. https://doi.org/10.1016/j.actbio.2020.09.024.

24. Zhang, B.; Cristescu, R.; Chrisey, D. B.; Narayan, R. J. Solvent-Based Extrusion 3D Printing for the Fabrication of Tissue Engineering Scaffolds. *Int. J. Bioprint.* **2020**, *6* (1), 19. https://doi.org/10.18063/ijb.v6i1.211.

25. Hou, X.; Huang, B.; Zhou, L.; Liu, S.; Kong, J.; He, C. An Amphiphilic Entangled Network Design Toward Ultratough Hydrogels. *Adv. Mater.* **2023**, *35* (28). https://doi.org/10.1002/adma.202301532.

26. Gao, D.; Wang, Z.; Wu, Z.; Guo, M.; Wang, Y.; Gao, Z.; Zhang, P.; Ito, Y. 3D-Printing of Solvent Exchange Deposition Modeling (SEDM) for a Bilayered Flexible Skin Substitute of Poly (Lactide-Co-Glycolide) with Bioorthogonally Engineered EGF. *Mater. Sci. Eng. C Mater. Biol. Appl.* **2020**, *112*, 110942. https://doi.org/10.1016/j.msec.2020.110942.

27. Han, C.; He, L.; Wang, Q.; Zhang, C. Solvent-Exchange-Assisted 3D Printing of Self-Polarized High β-PVDF for Advanced Piezoelectric Energy Harvesting. *ACS Appl. Electron. Mater.* **2022**, *4* (6), 3125–3133. https://doi.org/10.1021/acsaelm.2c00553.

28. Eom, W.; Hossain, M. T.; Parasramka, V.; Kim, J.; Sanders, K. A.; Piorkowski, D.; Lowe, A.; Koh, H. G.; Fudge, D. S.; Ewoldt, R. H.; Tawfick, S. H. Fast 3D Printing of Fine, Continuous, and Soft Fibers via Embedded Solvent Exchange. *Nat. Commun.* **2025**, *16* (1). https://doi.org/10.1038/s41467-025-55972-1.

29. Schwan, M.; Nefzger, S.; Zoghi, B.; Oligschleger, C.; Milow, B. Improvement of Solvent Exchange for Supercritical Dried Aerogels. *Front. Mater.* **2021**, *8*. https://doi.org/10.3389/fmats.2021.662487.

30. Kavda, S.; Golfomitsou, S.; Richardson, E. G. Effects of Selected Solvents on PMMA after Prolonged Exposure: Unilateral NMR and ATR-FTIR Investigations. *Herit. Sci.* **2023**, *11* (1). https://doi.org/10.1186/s40494-023-00881-z.

31. Mathur, A. M.; Hammonds, K. F.; Klier, J.; Scranton, A. B. Equilibrium Swelling of Poly(Methacrylic Acid-g-Ethylene Glycol) Hydrogels: Effect of Swelling Medium and Synthesis Conditions. *J. Controlled Release* **1999**, *54* (2), 177–184. https://doi.org/10.1016/S0168-3659(97)00186-7.

32. McBath, R. A.; Shipp, D. A. Swelling and Degradation of Hydrogels Synthesized with Degradable Poly(β-Amino Ester) Crosslinkers. *Polym. Chem.* **2010**, *1* (6), 860. https://doi.org/10.1039/c0py00074d.

33. Khalili, M. H.; Zhang, R.; Wilson, S.; Goel, S.; Impey, S. A.; Aria, A. I. Additive Manufacturing and Physicomechanical Characteristics of PEGDA Hydrogels: Recent Advances and Perspective for Tissue Engineering. *Polymers (Basel)* **2023**, *15* (10), 2341. https://doi.org/10.3390/polym15102341.

34. Bento, C. S. A.; de Sousa, H. C.; Braga, M. E. M. Measurement of Ethanol Concentration for Monitoring the Solvent Exchange during the Alcogel Preparation. *MethodsX* **2024**, *13*, 102960. https://doi.org/10.1016/j.mex.2024.102960.

35. Gurikov, P.; S. P., R.; Griffin, J. S.; Steiner, S. A.; Smirnova, I. 110th Anniversary: Solvent Exchange in the Processing of Biopolymer Aerogels: Current Status and Open Questions. *Ind. Eng. Chem. Res.* **2019**, *58* (40), 18590–18600. https://doi.org/10.1021/acs.iecr.9b02967.

36. Bailey, B. M.; Hui, V.; Fei, R.; Grunlan, M. A. Tuning PEG-DA Hydrogel Properties via Solvent-Induced Phase Separation (SIPS). *J. Mater. Chem.* **2011**, *21* (46), 18776. https://doi.org/10.1039/c1jm13943f.

37. Arabi, S. H.; Haselberger, D.; Hinderberger, D. The Effect of Ethanol on Gelation, Nanoscopic, and Macroscopic Properties of Serum Albumin Hydrogels. *Molecules* **2020**, *25* (8), 1927. https://doi.org/10.3390/molecules25081927.

38. Liu, R.; Qin, P.; Wang, L.; Zhao, X.; Liu, Y.-H.; Hao, X. Toxic Effects of Ethanol on Bovine Serum Albumin. *J. Biochem. Mol. Toxicol.* **2010**, *24* (1), 66–71. https://doi.org/10.1002/jbt.20314.

39. Calvert, P. Hydrogels for Soft Machines. *Adv. Mater.* **2009**, *21* (7), 743–756. https://doi.org/10.1002/adma.200800534.

40. Ngo, T. D.; Kashani, A.; Imbalzano, G.; Nguyen, K. T. Q.; Hui, D. Additive Manufacturing (3D Printing): A Review of Materials, Methods, Applications, and Challenges. *Compos. B Eng.* **2018**, *143*, 172–196. https://doi.org/10.1016/j.compositesb.2018.02.012.

41. Ligon, S. C.; Liska, R.; Stampfl, J.; Gurr, M.; Mülhaupt, R. Polymers for 3D Printing and Customized Additive Manufacturing. *Chem. Rev.* **2017**, *117* (15), 10212–10290. https://doi.org/10.1021/acs.chemrev.7b00074.

42. Formlabs. Post-Processing and Finishing SLA Prints. Formlabs Blog. Available at: https://formlabs.com/blog/post-processing-and-finishing-sla-prints/ (accessed April 6, 2025).

43. Gibson, I.; Rosen, D.; Stucker, B. *Additive Manufacturing Technologies*; Springer: New York, NY, **2015**. https://doi.org/10.1007/978-1-4939-2113-3.

44. Murayama, K.; Tomida, M. Heat-Induced Secondary Structure and Conformation Change of Bovine Serum Albumin Investigated by Fourier Transform Infrared Spectroscopy. *Biochemistry* **2004**, *43* (36), 11526–11532. https://doi.org/10.1021/bi0489154.

45. Sanaeifar, N.; Mäder, K.; Hinderberger, D. Macro- and Nanoscale Effect of Ethanol on Bovine Serum Albumin Gelation and Naproxen Release. *Int. J. Mol. Sci.* **2022**, *23*, 7352. https://doi.org/10.3390/ijms23137352.